*MAT_4A_MICROMEC – Theory and Application notes

P. Reithofer[1], A. Fertschej[1], B. Hirschmann[1], B. Jilka[1], A. Erhart[2], S. Hartmann[2]
(1) 4a engineering GmbH, (2) DYNAmore GmbH

Abstract

Nowadays a great number of short and long fiber reinforced thermoplastics play a decisive role in the automotive industry to ensure affordable lightweight design and availability in large quantities. As seen in the last German LS-DYNA Conference 2016, there is a strong industry interest to consider the manufacturing process induced local anisotropy in crash and general dynamic simulations.

Looking at material models only homogenized macroscopic composite material laws have been available in LS-DYNA® (e.g. ***MAT_157**). Starting with the actual LS-DYNA® Release R10 a new micromechanically based material model ***MAT_215/ *MAT_4A_MICROMEC** is available, which should simplify simulation process chains and provide more accurate simulation results.

Current investigations on different plastic materials deal with **M**aterial **P**arameter **I**dentification **P**rocedures for ****MAT_215***. Besides further validation of the anisotropic material deformation behavior failure prediction of different polymer grades by using the implemented features is work in progress. Furthermore, the influence of material parameters on the structural behavior will be shown and the steps from standard laboratory tests to studies on part level domain will be shown.

Introduction

For 30 years aerospace and sports industries have been using anisotropic material models in their product development. A relative conservative development process is typical for those industries, stiffness and integrity of operation are the main simulation tasks. Therefore, one will find appropriate material models in all well-known implicit commercial solvers (e.g. Abaqus®, Ansys®, Nastran®...).

The demand of weight reduction in the automotive industry has led to a strong interest in various composite applications. In the case of classical composites (e.g. carbon, glass, kevlar, endless reinforced materials ...) the focus in material model development was the failure prediction and the post failure energy consumption. Recent developments in LS-DYNA® are initiated due to the need of crash simulation applications. The properties of composite materials are often highly influenced through the manufacturing process, typically injection molding in case of short (SFRT) and long fiber reinforced thermoplastics (LFRT). The fiber orientation is developing through the extensional and shear flow in the mold (fig. 1).

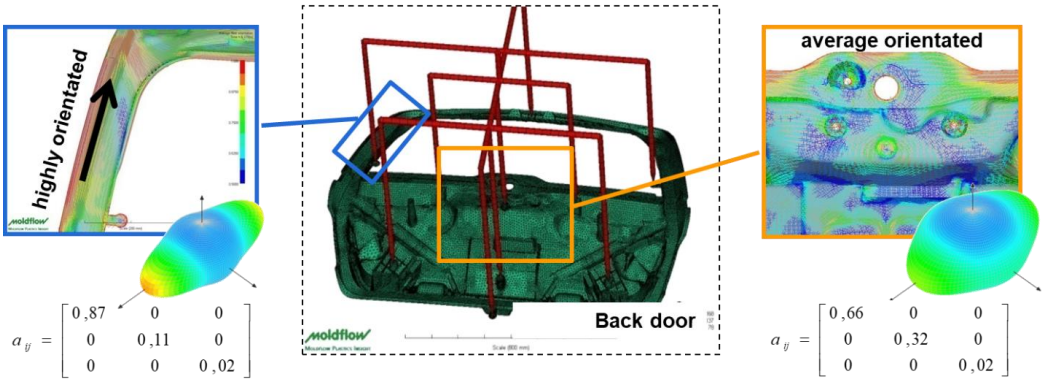

Fig.1: Typical fiber orientation through the thickness in an injection molded part [1].

Material behavior of SFRT and LFRT

Fiber size, geometry, content, and orientation have a very significant influence on the part performance. Following figures give a short overview of the mechanical material behavior of SFRT generated by 3-point-bending tests. The dynamic tests were carried out on the testing device IMPETUS™, which was developed for dynamic material characterization and fast reliable material card generation [2].

Fig. 2 shows the influence of the **glass fiber** on the mechanical behavior. The **"anisotropy"** of the properties increases with increasing alignment of the fibers (left) and content (right). Fig. 3 demonstrates the influence of the **polypropylene matrix** on the composite material behavior. The viscoelasticity and -plasticity of the thermoplastic matrix are more pronounced in the transversal direction measurements of the composite (figure 3, left). Also, a strong dependency on the temperature can be seen especially for the failure behavior (figure 3, right); the test specimens become more brittle with decreasing temperatures.

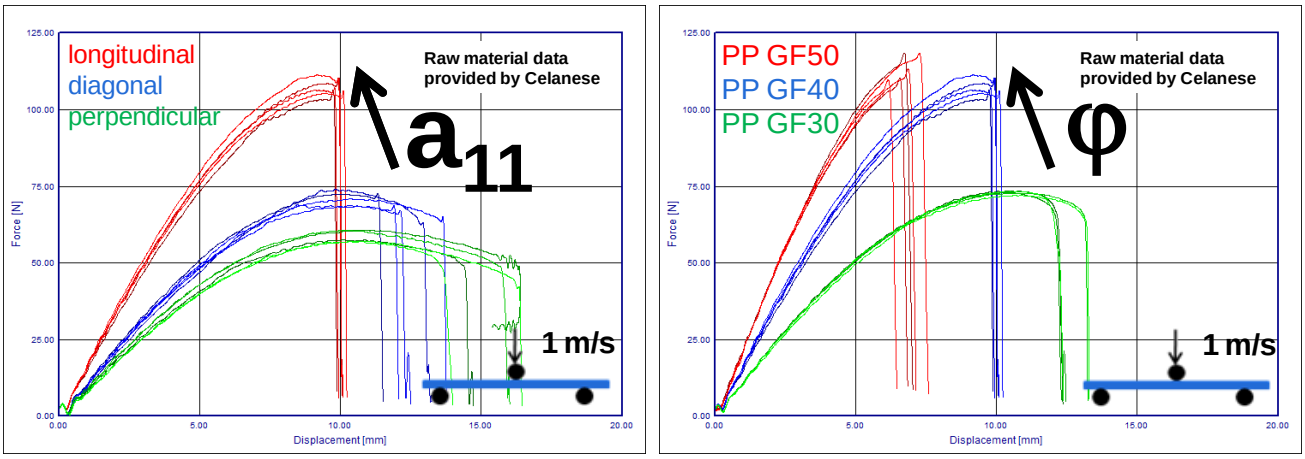

Fig.2: Influence of fiber orientation (left – PPGF40) and fiber content (right - longitudinal) shown by the force-displacement curves for fiber reinforced PP tested in a 3-point-bending test using IMPETUS™ [3].

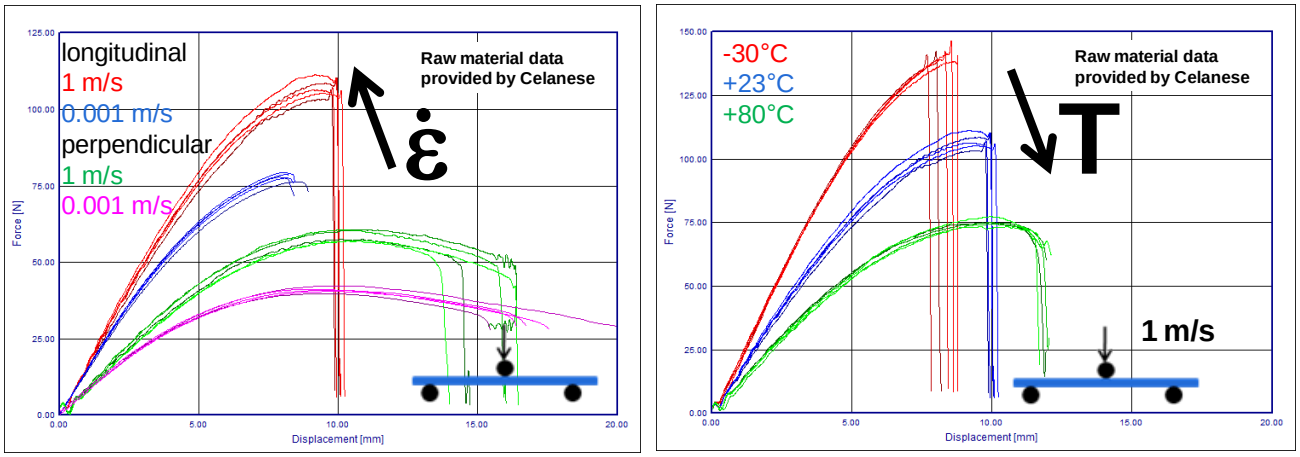

Fig.3: Influence of strain rate dependency (left – PPGF40) and temperature (right– PPGF40 longitudinal) demonstrated by the force-displacement curves for a reinforced PP tested in a 3-point-bending test [3].

Material models – State of the art

A huge number of constitutive models for anisotropic materials are implemented in various solvers. These models are able to consider anisotropic influences on some extent. Table 1 shows some material models of LS-DYNA®. Depending on the requirements of the application (e.g. considering plasticity, damage, failure) the material model that suits best should be chosen.
In the case of "classic" endless fiber reinforced composites, the common solvers offer orthotropic elasticity in combination with orthotropic failure criteria (Chang/Chang, Tsai-Wu, Puck ...) and damage models. The anisotropic viscoelastic and viscoplastic material behavior of SFRT/LFRT can currently be considered in most common solvers by using orthotropic elasticity in combination with HILL plasticity. Having a quick look into the LS-DYNA® user's manual, one will find that at least 20 material model parameters have to be determined by material testing, before this model can be used in daily work.

Table 1: Standard material models for anisotropic materials available in LS-DYNA® [4], [5].

No.	Elastic	Plastic	Damage	Strain rate	Failure	
2	**Ortho / Anisotropic**	**None**	**None**	**None**	***MAT_ADD_EROSION**	**SFRT / LFRT**
24	Isotropic	Mises	None	Plasticity	*MAT_ADD_EROSION	
103	Isotropic	Hill	None	Plasticity	*MAT_ADD_EROSION	
108	Orthotropic	Hill	None	None	*MAT_ADD_EROSION	
157	**Anisotropic**	**Hill**	**None**	**Plasticity**	Tsai-Hill/Tsai-Wu & ***MAT_ADD_EROSION**	
215	***MAT_4A_MICROMEC available since R10: Model based on MORI TANAKA MEANFIELD**					
22	Orthotropic	None	None	None	Orientation dependent	**Carbon, Glass, Kevlar endless & fabric**
54/55	Orthotropic	Pseudo	None	Strength	Chang-Chang/ Tsai-Wu Orientation dependent	
58	Orthotropic	None	Elastic Orthotropic	Strength, Stiffness	mod. Hashin Orientation dependent	
158	Orthotropic	None	Elastic Orthotropic	viscoelasticity	Orientation dependent	
261	Orthotropic	In plane shear	Elastic Orthotropic	Strength	failure Pinho (Puck) Orientation dependent	
262	Orthotropic	In plane shear	Elastic Orthotropic	Strength, Fracture toughness	failure Camanho (Puck) Orientation dependent	

Typical explicit simulation applications would be drop tests of consumer goods or pedestrian/occupant safety tests in the automotive industry. Typically, isotropic elastic and viscoplastic material models (e.g. ****MAT_024*** in LS-DYNA®) are used for the idealization of these highly anisotropic materials. As shown in figure 4, three material cards as best/worst case (longitudinal/perpendicular) and average case (diagonal) are built from tensile (classical approach) or bending (IMPETUS™ - VALIMAT™ approach) tests.

Shorter development times, the vast amount of different polymer grades used, the extensible material card parameter determination, and also the simulation time consumption are comprehensive reasons to use the simple approach with isotropic material models as described before. Nevertheless, to predict failure the local anisotropy has to be considered. Therefore, a new approach was developed to fulfill the requirement of **favorable** (time and costs) and **reliable** (local anisotropy) material characterization.

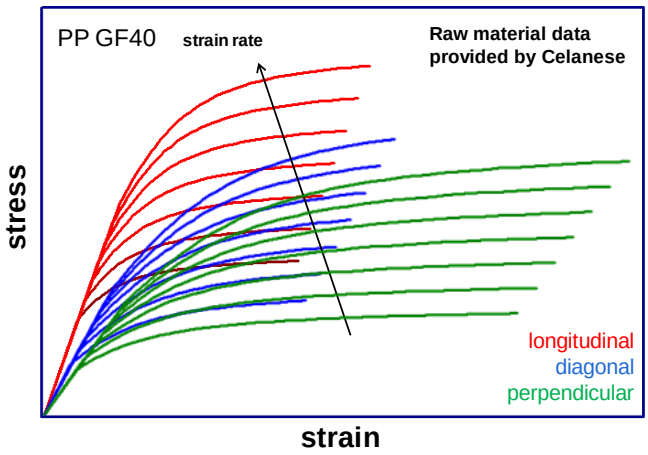

*Fig.4: Stress-strain curves for three directions of a ***MAT_024** material card generated with the reverse engineering VALIMAT™ approach [2], [3].*

As mentioned before, fiber orientation influences the mechanical material behavior of SFRT. The fiber orientation itself is influenced by the injection molding process. Near the surface the fibers are mainly oriented in flow direction, while in the middle of the part the fiber orientation is perpendicular to the flow direction. In the bending test the (higher) fiber orientation close to the surface plays a more important role in the result compared to a tensile test. As the bending case is the most common load case for the application, a material characterization using bending tests is rewarding and advantageous.
Specimens for the material characterization itself are also affected by the molded plaques (e.g. tensile bar, quadratic or rectangular plaque, thickness of plaque ...) and **will never** cover all possible fiber orientations that will occur in a real part. Figure 5 shows the influence of the resulting fiber orientation tensor on the tensile behavior in flow and perpendicular to the flow direction [6].

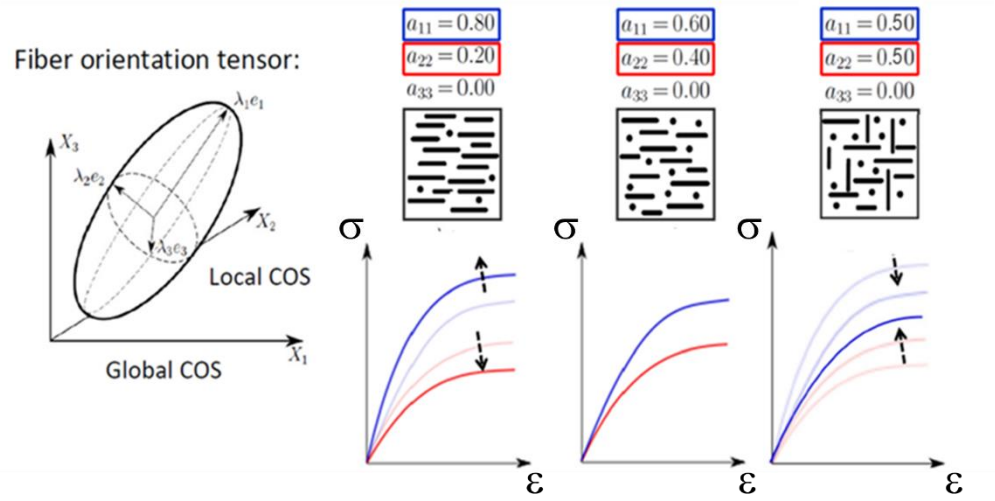

Fig.5: Influence of the fiber orientation tensor on the stress strain behavior [6].

It is obvious that without any micro-mechanical approach one will not be able to determine all these parameters in dependence of the process induced local fiber orientation.

Starting point of the micro mechanical approach is the rule of mixture for averaging the stresses σ and strains ε

$$\bar{\sigma}^{C} = \varphi\bar{\sigma}^{F} + (1-\varphi)\bar{\sigma}^{M} \text{ and } \bar{\varepsilon}^{C} = \varphi\bar{\varepsilon}^{F} + (1-\varphi)\bar{\varepsilon}^{M}. \quad (1)$$

where C...composite, F...fiber, M...matrix.

Central point of the mean field theory is that the average stress σ^F and strain ε^F in the inclusion can be calculated from the average stress σ^M and strain ε^M in the matrix [7, 8]. This can be expressed through

$$\underline{\bar{\sigma}}^{F} = \underline{\underline{B}}^{\sigma}\,\underline{\bar{\sigma}}^{M} \text{ and } \underline{\bar{\varepsilon}}^{F} = \underline{\underline{B}}^{\varepsilon}\,\underline{\bar{\varepsilon}}^{M}. \quad (2)$$

B denotes the so-called concentration tensor. Under elastic conditions

$$\underline{\bar{\sigma}}^{F} = \underline{\underline{S}}^{F}\,\underline{\bar{\varepsilon}}^{F} \text{ holds, therefore } \underline{\underline{B}}^{\sigma} = \underline{\underline{S}}^{F}\,\underline{\underline{B}}^{\varepsilon}\,\underline{\underline{C}}^{M}, \text{ whereby } \underline{\underline{C}}^{M} = \left(\underline{\underline{S}}^{M}\right)^{-1} \quad (3)$$

in which S is the stiffness, C the compliance tensor for the individual component. B can be calculated analytically for ellipsoidal inclusions using Eshelby´s solution [9, 10].

Using the software solution MICROMEC™ [11], the 3D thermoelastic properties of a fiber reinforced material can be calculated rapidly. Like Digimat-MF®, MICROMEC (see figure 6**Fehler! Verweisquelle konnte nicht gefunden werden.**) is based on the **Mori Tanaka Meanfield Theory**.

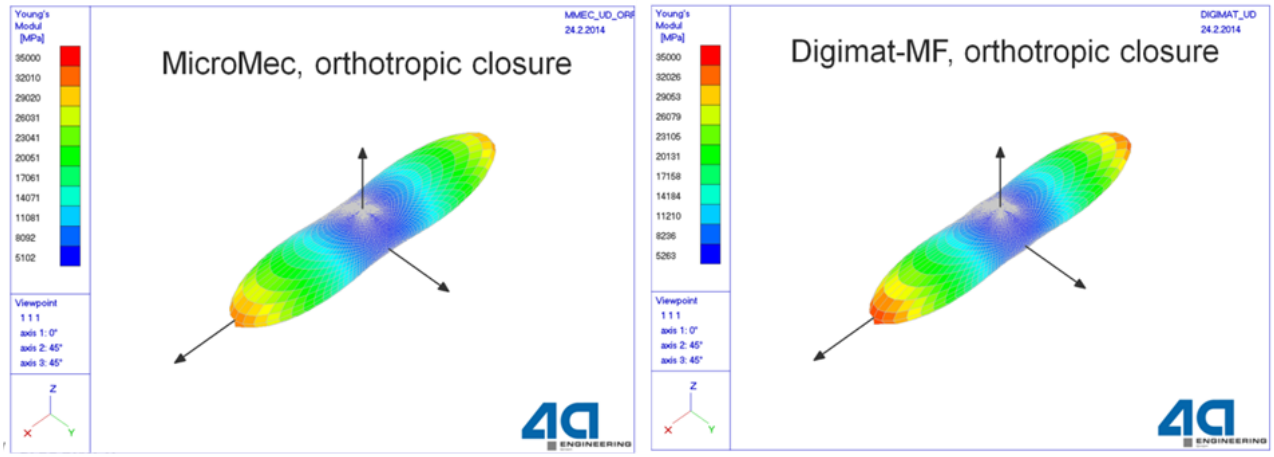

Fig.6: Comparison between Digimat-MF® and MICROMEC™ - identical results [12].

Not only this homogenization of the material properties is one of the main advantages using micro mechanical models, but also the differentiation of fiber and matrix strains and stresses. In a material model this can be used to trigger plasticity on the matrix or to trigger failure and damage models either on matrix or fiber. Mlekusch et al. [13] show how this can be used to develop a failure criterion based on matrix equivalent stresses.

Recent developments in the software solutions VALIMAT™ (former 4a impetus) [14] are including MICROMEC™ as library for the direct use in parameter identification. For the reverse engineering process, the number of design variables for an anisotropic elastic and viscoplastic material card will be reduced from the above mentioned 20 to 3-5 which is equivalent to the normal isotropic approach.

Material Model *MAT_215 (*MAT_4A_MICROMEC)
Historical and Theoretical Background

To improve the current state of the art 4a provided DYNAmore a LS-DYNA® usermaterial to be implemented as a standard LS-DYNA® material model. Based on [15] the core functionality to calculate the thermoelastic composite properties using the Mori Tanaka Meanfield Theory, can be found in the software product MICROMEC™. Based on the material knowledge of fiber reinforced plastics in the past 15 years this model was extended to an elasto-viscoplastic matrix behavior. The developments focused on the essential known mechanical material behavior, which leads to a fast and robust material model. Fiber failure may be considered with a simple maximum stress criterion. Matrix failure was implemented as damage initiation and evolution model (DIEM), optional also as composite strain based criterion available [16]. The main framework of the material model can be found in figure 7.

$$\Delta\varepsilon^C \Rightarrow \Delta\varepsilon^M, \left(\Delta\varepsilon^F\right)$$
$$\Delta\varepsilon^M = \frac{1}{\varphi\overline{B_i} + (1-\varphi)I}\Delta\varepsilon^C$$
$$\Delta\varepsilon^M \Rightarrow E_M^T, \Delta\varepsilon^M{}_{pl}, \Delta\sigma^M$$
$$\overline{B}_{i+1} = f\left(fo^{(4)}, E_M^T, l/d\right)$$
$$\overline{A} = S^F\,\overline{B}_{i+1}C^M$$
$$\Delta\sigma^C = \left[\varphi\overline{A} + (1-\varphi)I\right]\Delta\sigma^M$$

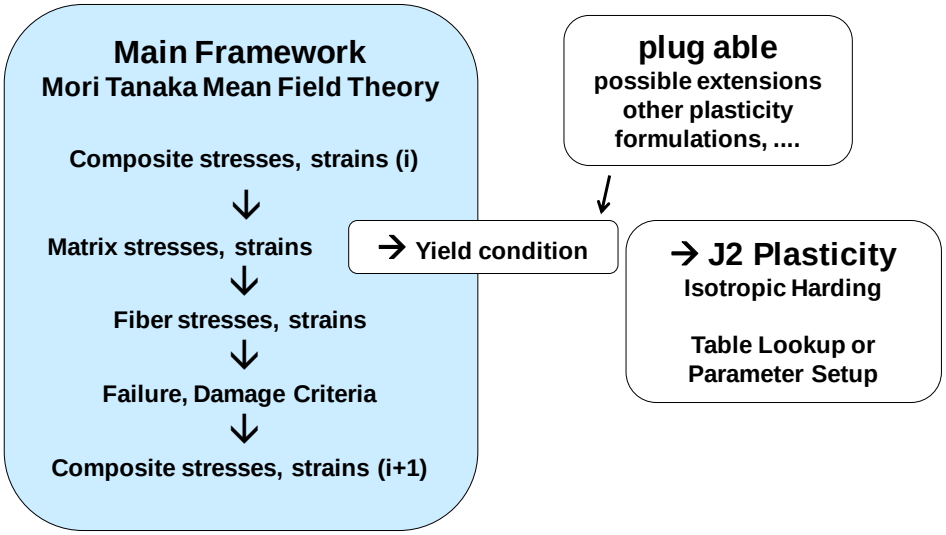

Fig.7: Main framework implemented for ****MAT_215/*MAT_4A_MICROMEC****.*

The required keyword input properties can be seen in fig. 8. Starting with R10 the presented material model is available as ***MAT_215/*MAT_4A_MICROMEC**, implemented for shell, thick shell and solid elements.

```
$=========================================================================
*MAT_4A_MICROMEC
$01     mid      mmopt       bupd         --         --      failm      failf     NUMINT
   1000000        1.0       0.01                               0.         0.      -65.
$02    aopt       macf         xp         yp         zp         a1         a2         a3
          0          0        0.0        0.0        0.0        1.0        0.0        0.0
$03      v1         v2         v3         d1         d2         d3       beta         --
         0.0        0.0        0.0        0.0        0.0        1.0       45.
$04     fvf         --         fl         fd         --        a11        a22         --
        .115                   53.        1.0                   .7        .25
$05     rof         el         et        glt       prtl       prtt         --         --
2.5899e-09      70000.     70000.     28759.      0.217      0.217
$06      xt         --         --         --         --         --     SLIMXT     NCYRED
      2800.                                                            0.01         10
$07     rom          e         pr         --         --         --         --         --
  1.09e-09      1500.        0.3
$08   sigyt      etant         --         --       eps0          c
$09    LCST         --         --         --       LCDI       UPF
   1000000                                    1000020  -1000026
$=========================================================================
```

header — options, direction
composite — definition
fiber — transversal i. elasticity, failure
matrix — isotropic elasticity, viscoplasticty, damage

Fig.8: Typical keyword input for ****MAT_215/*MAT_4A_MICROMEC.***

Verification

To test the new implemented material model some 1-Element verification examples were conducted. Focusing on the elasticity fig. 9 shows a comparison between ***MAT_022** and ***MAT_215** for some extreme material card parameter values: 100% matrix, 100% fiber (isotropic and transversal isotropic) and a 60vol% endless fiber composite composition for different orientations under pure tension load.
Investigating the element formulation (shell type 16 and solid type 2), a SFRT PA6 GF30 material was used to verify the elasticity under different loading directions, the same expected results are shown in fig. 10.
To test the visco-plasticity part of the material model, 1-Element tests for different loading velocities were performed, see fig. 11. To check the robustness of the general material model a full factorial DOE in LS-OPT® by varying fiber mass fraction, fiber length and orientation and loading direction was conducted. All 1008 1-Element tests run through without an error termination.

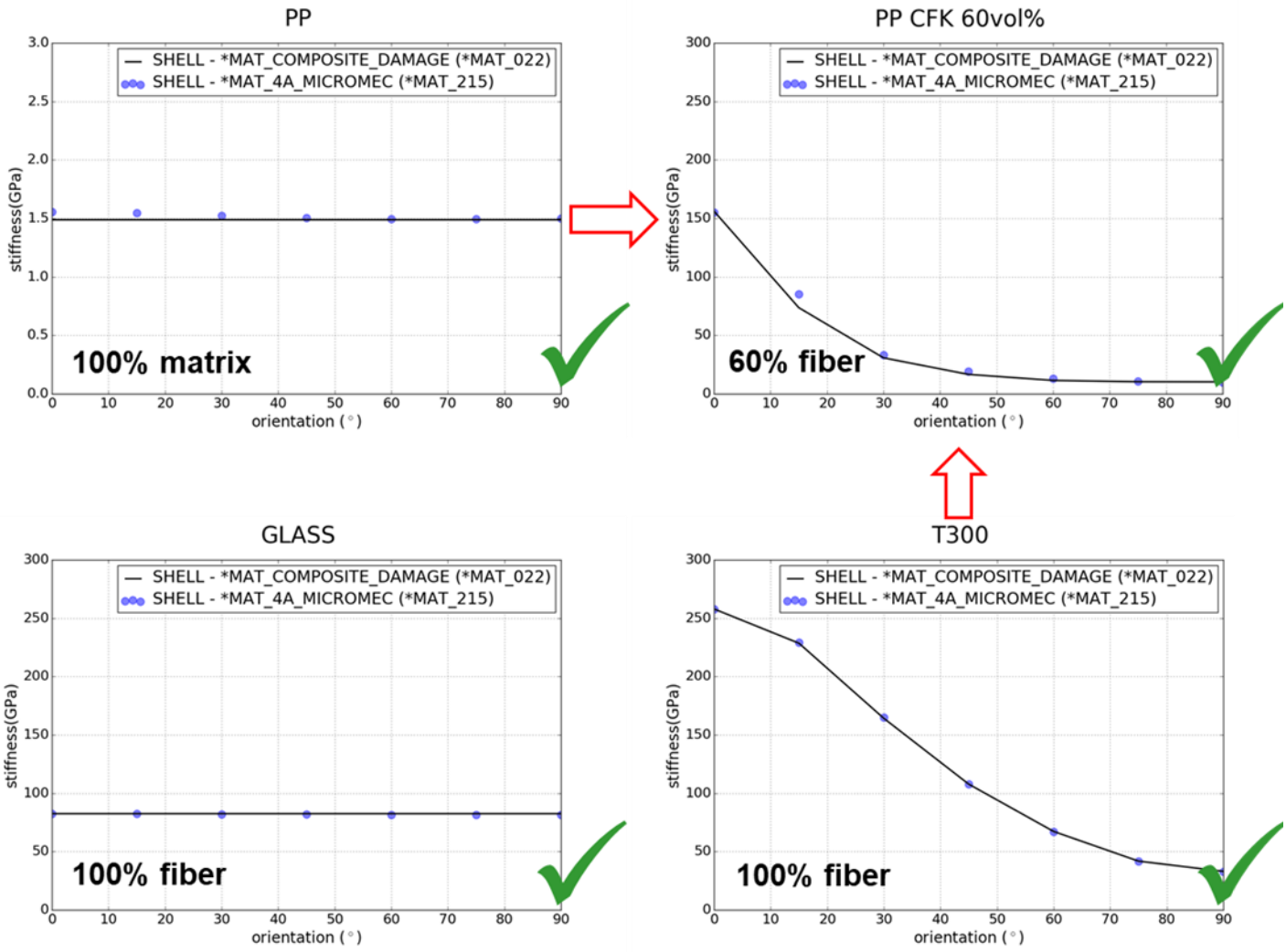

Fig.9: Verification by 1-Element tension tests under different loading directions (orientation): pure PP matrix (left top), pure glass fiber (left bottom), pure T300 fiber (right bottom), Composite 60% volume fraction T300 in PP matrix (right top).

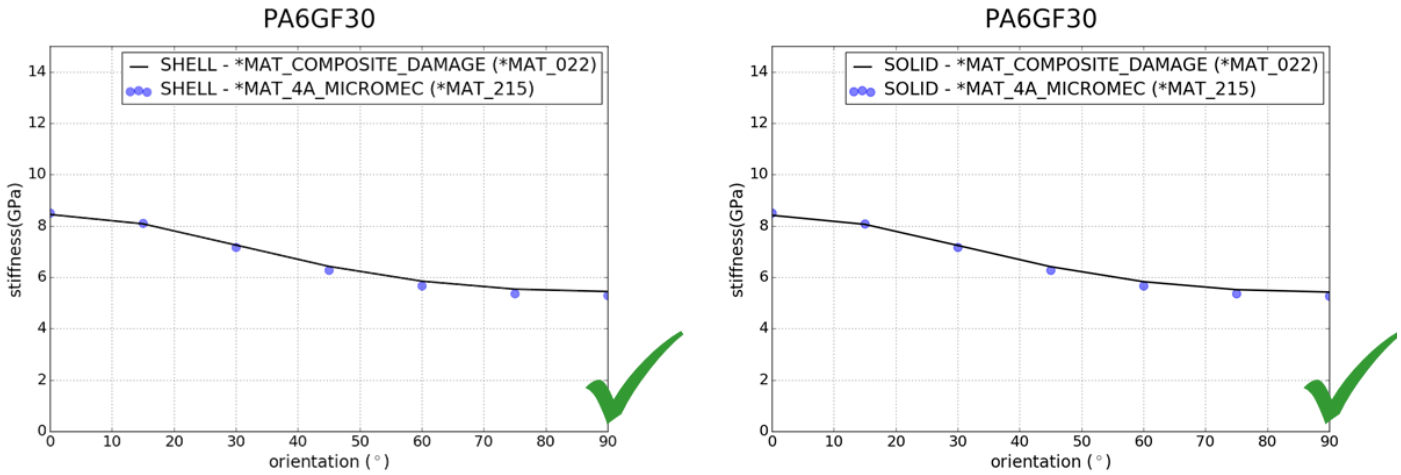

Fig.10:Verification of ****MAT_215*** *- 1-Element tension test under different loading directions (orientation): Shell TYPE 16 (left), Solid TYPE 2 (right)*

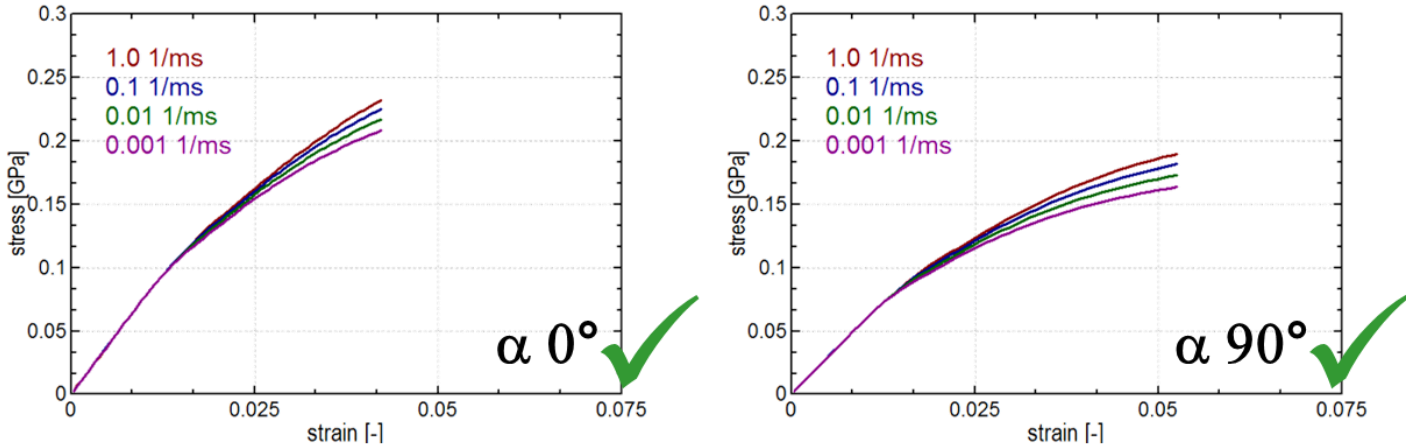

Fig.11:Verification of ****MAT_215*** *- 1-Element tension test under different loading velocities: longitudinal – 0° (left), transversal – 90° (right)*

DOE with LS-OPT:

MATRIX:	PP
FIBER:	GLASS
FVF:	-0.05;-0.15;-0.20;-0.25;-0.30;-0.35;-0.40;-0.50;-0.60
FL:	100;200;500;1000
A11:	0.6;0.7;0.8;0.9
α:	0°;15°;30°;45°;60°;75°;90°

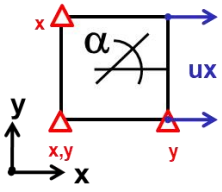

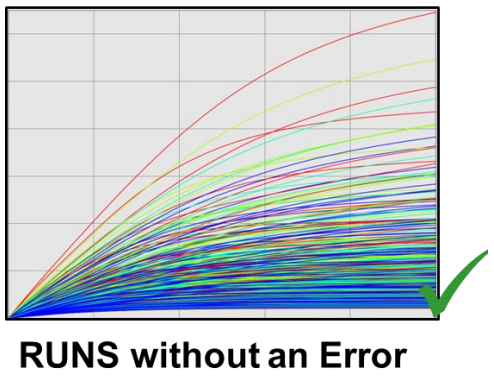

Fig.12:Verification of ****MAT_215*** *-1-Element* ***DOE with LS-OPT***

Material Characterization / Validation

For more than 15 years 4a is working on and performing material characterization of plastics and composites. The starting point was the development of an efficient dynamic testing system – the so-called IMPETUS™ - to generate validated material cards for explicit simulations mainly based on bending load cases (see fig. 13). VALIMAT™ can be used to semi-automatically generate validated material cards out of conducted tests. A good overview of our capabilities and newest developments can be found in [17].

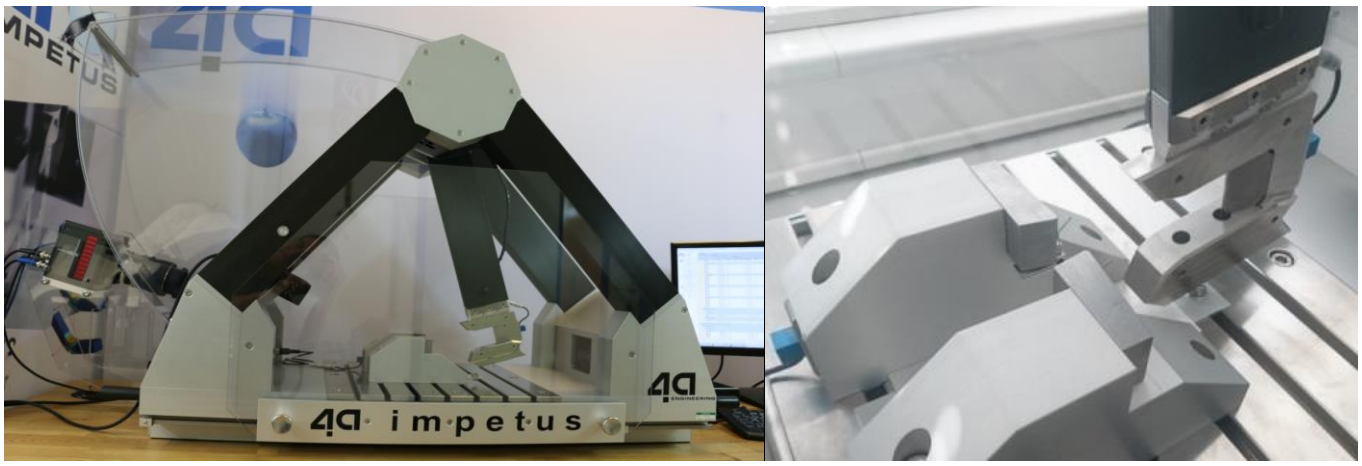

Fig.13:left - actual version of IMPETUS™, right - test setup bending

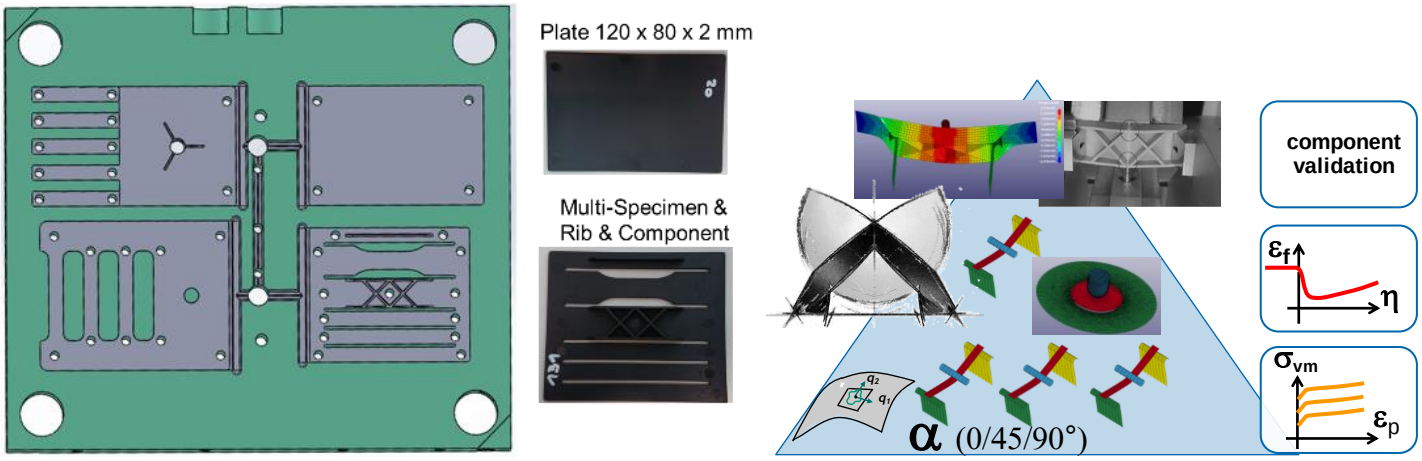

Fig.14:left - Injection molding: used mold for material characterization [18];
right - Material characterization pyramid for fiber reinforced plastics

To get high quality material cards one needs a concept,

- starting with molding adequate plaques for material characterization (fig.14 left)
- over characterizing the basic deformation and failure behavior in a standardized workflow (fig.14 right)
- up to finally validating the so obtained material card on component level.

Several SFRT and LFRT materials (e.g. PA6GF30, PPGF30, PBTGF30) were already successfully characterized by this concept [18], [19].

For the coupon level different samples are cut out in different orientations and tested for main loading cases (uniaxial and biaxial tension). The fiber orientation can be considered by mapping results of injection molding simulations or µCT measurements. Alternatively, an engineering approach could be, to divide one's simulation model in a core–skin-core layup over thickness with typical known fiber orientation values [20]. These concepts are supported by 4a software tools FIBERMAP™ respectively VALIMAT™ [21].

For thermoplastic materials, the assumption that failure only occurs under positive triaxiality values leads to the ductile criterion curve shown in figure 15, for details see [22].

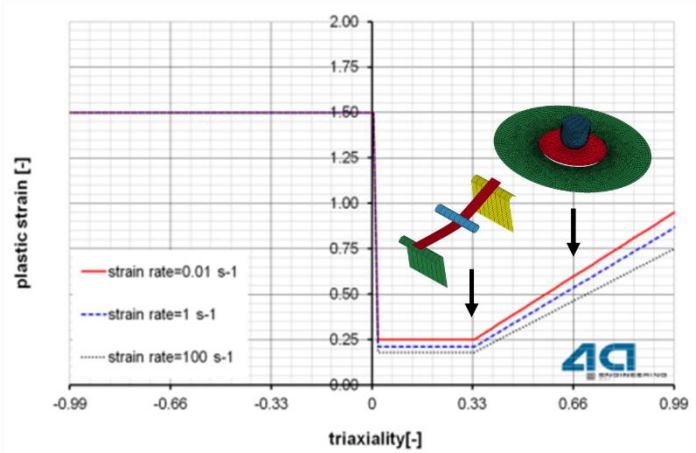

Fig.15: Example of failure curves in dependence of triaxiality and strain rate.

Static and dynamic 3-point-bending and puncture tests can be used to calibrate the damage and failure criteria. Exemplary validation results (force-displacement) for a PPGF30 material are shown in figure 16 and 17. In the bending case for different specimen orientation one can see the good correlation between simulation (solid line) results and average test (dotted line) curves. In the right figure the comparison for the puncture test is shown, the agreement between measured and simulated force-displacement curve is not quite well. Reasons could be that the failure mechanism could not be covered by the used shell idealization (TYPE 16). In case of using solid elements the failure mechanism in the puncture case can be captured quite well (figure 18).

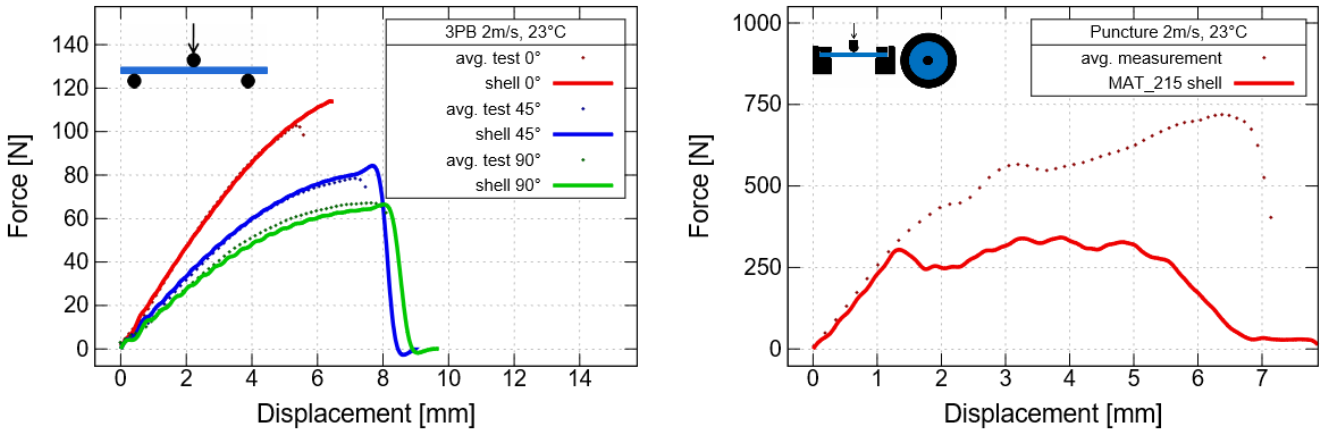

Fig.16: Validation results – Shell TYPE16: left – dynamic bending for specimen cut out of a plaque under different orientations; right – dynamic puncture test also conducted on IMPETUS™.

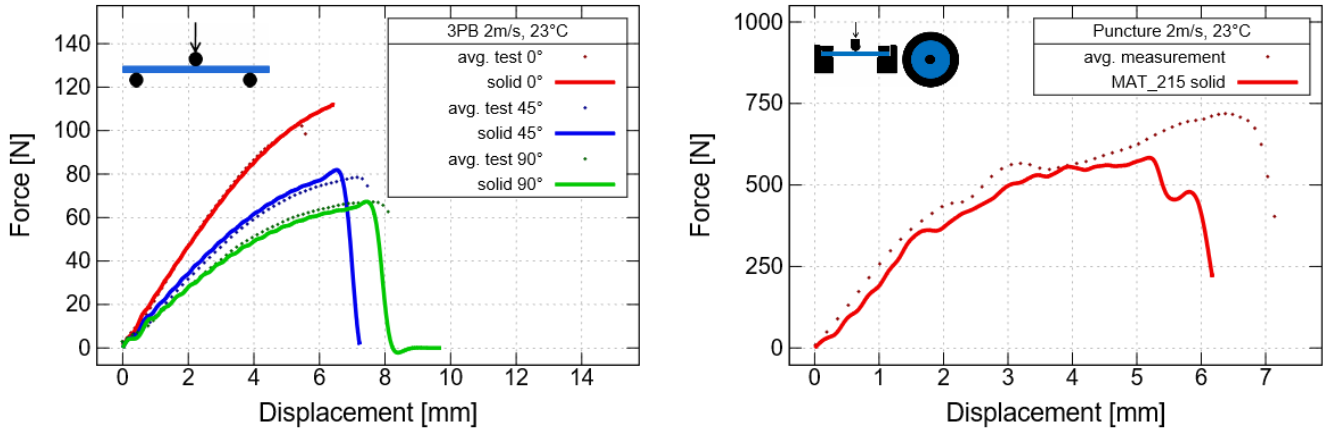

Fig.17: Validation results – Solid TYPE4: left – dynamic bending for specimen cut out of a plaque under different orientations; right – dynamic puncture test also conducted on IMPETUS™.

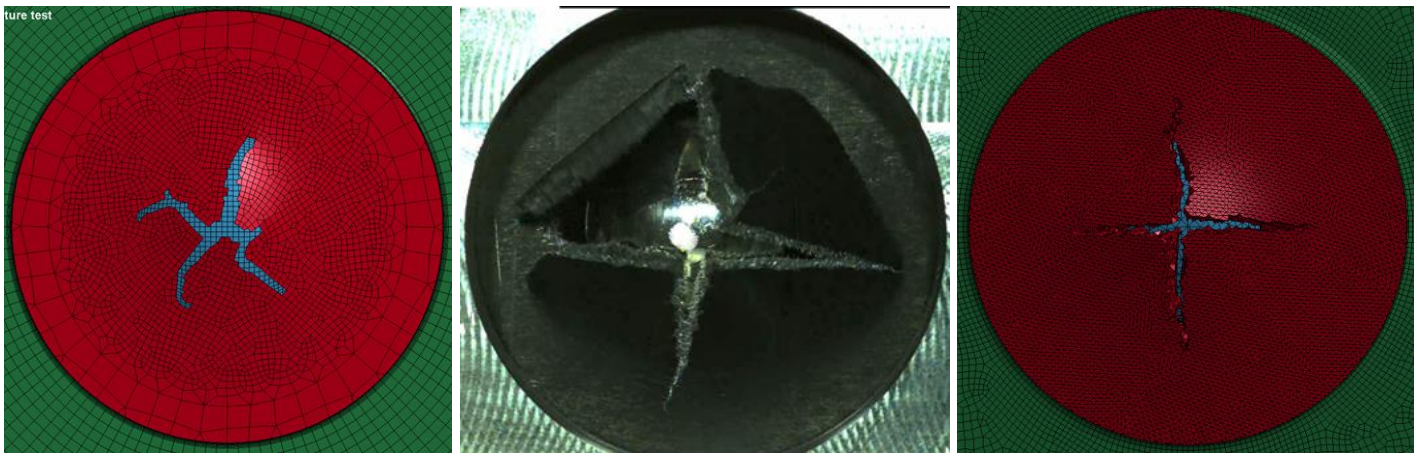

Fig.18: Failure under biaxial loading, in case of fine solid idealization (0.5 mm) good matching between test and simulation; left – simulation with shells, middle – test, right – sim. with solids

Finally, a component test "XX-rib" was conducted as well as the simulation of the same test including the integrative simulation process chain, meaning mapping of the fiber orientation: Autodesk Moldflow® → FIBERMAP™ → LS-DYNA®. Figure 19 shows good matching between measured and simulated force-displacement curves.

To summarize - while covering the deformation behavior is quite straight forward, the first failure behavior can be captured quite promising by using ***MAT_215**. Current investigations focus on failure modelling, especially how to improve the post failure under biaxial loading for shell elements.

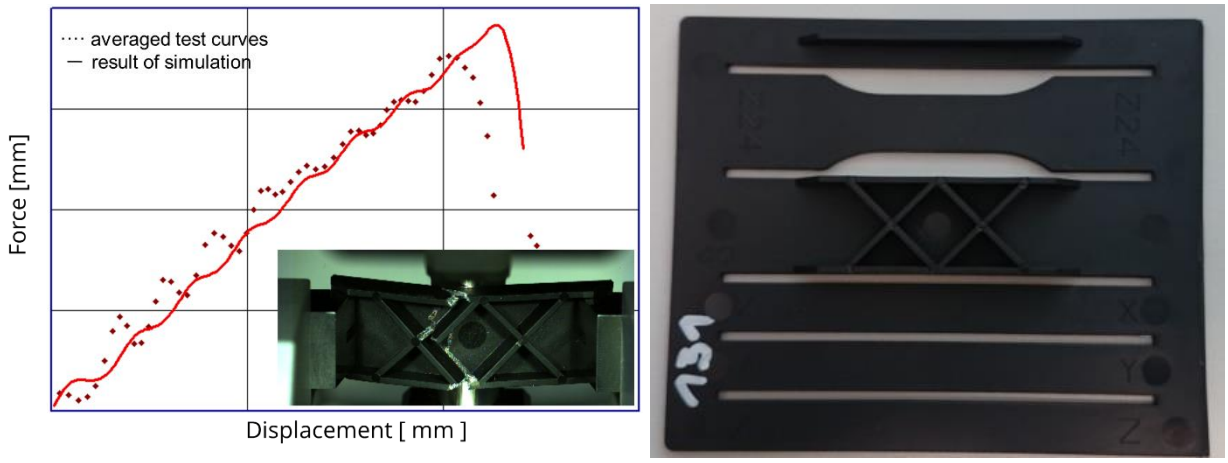

Fig.19:left - Validation result XX-rib under dynamic loading; right – specimen plaque including XX-rib

Application Notes / Case Studies / CPU consumption

In this contribution the results of two case studies are summarized. First case study is an automotive part, a so-called sleeve kindly provided by Hirtenberger Automotive Safety GmbH & Co KG. The provided LS-DYNA® model had about 470.000 tetrahedron elements, the filling simulation was done with Moldex3D® and the resulting fiber orientation was mapped with FIBERMAP™ (fig. 20). In the keyword file the orientation was covered by using ****ELEMENT_SOLID_ORTHO***. The real part was tested in a fall tower, force-displacement was measured, a high-speed camera recorded the failure development of the component. Fig. 21 shows the test results as well as a simulation comparison between the approach using an isotropic material model ****MAT_024*** and the integrative approach with a fully anisotropic material model ****MAT_215*** as described before. As one can see only by considering the local, process induced fiber orientation the deformation as well as the failure behavior of the tested part is covered well in the simulation. Using an isotropic material model, the part fails on a completely different location. For more details on this research project refer to [21], [23].

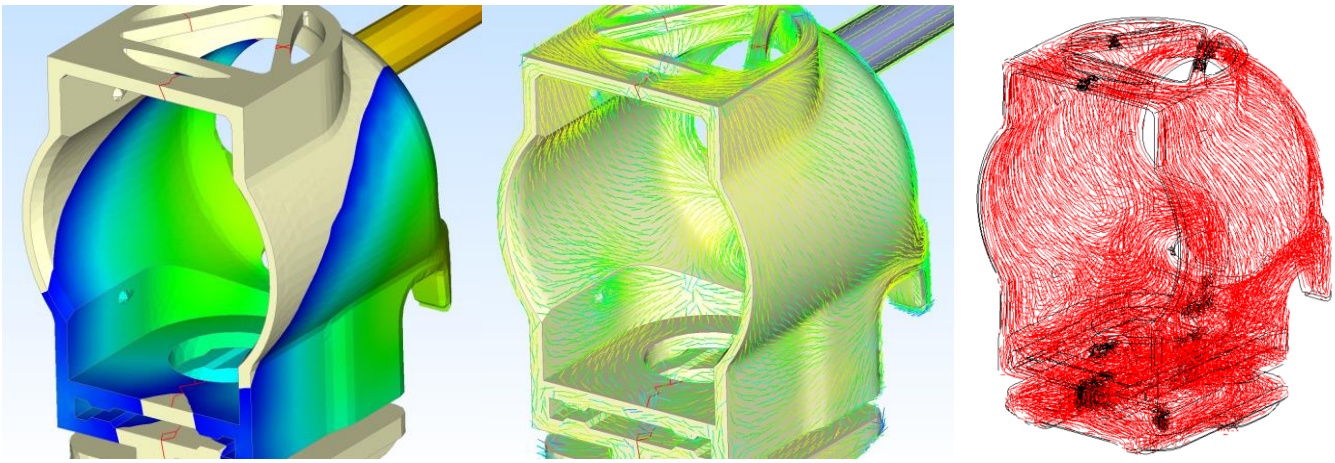

Fig.20:left – filling of the sleeve in Moldex3D®; middle – fiber orientation result in Moldex3D, right – assigned orientation in the final input deck.

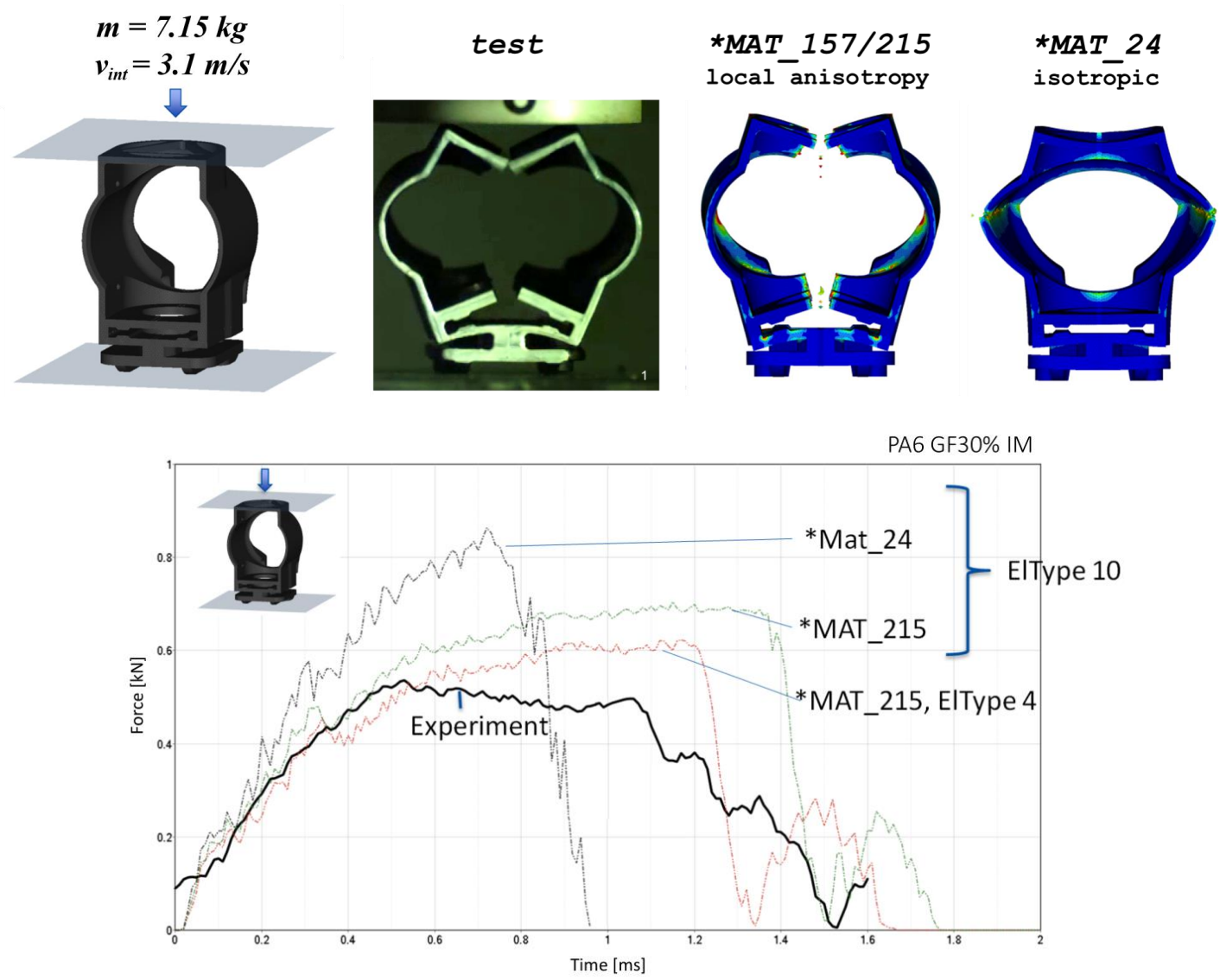

Fig.21:Results of the case study "sleeve" presented in [23].

A second case study is based on the publication of Bosch Automotive Products (Suzhou) Co., Ltd. In this paper investigations on drop tests of a fiber reinforced automotive control unit were conducted and the usage of isotropic vs. anisotropic material models was compared. The outcome showed the usefulness of an adequate material model in combination with integrative simulation as it can not only predict crack location correctly, but also shows very good correlation of the critical drop height between simulation and experimental results [18].
These investigations using ***MAT_157** were done with more than 700.000 tetrahedron elements. For validation purpose as well as cross-check for material model performance the LS-DYNA® model was simulated with ***MAT_024** and ***MAT_215**. The measured increase in CPU-time was about **~1.7 (20 vs 32 hours).**

Summary & Outlook

To increase the prediction quality for SFRT and LFRT materials in explicit simulations an anisotropic material model has to be taken into account. In the last years such an anisotropic elastic visco-plastic material model based on the Mori Tanaka Meanfield theory was developed and implemented in the commercial FEM Solver LS-DYNA®. The micromechanical approach separates composite stress and strains into its matrix and fiber components. Fiber orientation is a direct input for the model and can therefore be easily assigned by a mapping software, that allows an ease of use of the material model. Failure of the material is considered by a damage initiation evolution model (DIEM) for the matrix, also a simplified maximum stress criterion for the fiber was implemented in the model.

Verification tests in the elastic domain were performed by comparing ***MAT_215** to ***MAT_022**, which showed good matching. A DOE for fiber content, orientation and length as parameters in a PP matrix to investigate the visco-plastic domain was also conducted, more than 1000 simulation runs succeeded without convergence problems.

Furthermore, a material characterization procedure was introduced and tested on several SFRT and LFRT materials, to determine the required input parameters for the material model. While covering the deformation behavior is quite straight forward, the first failure behavior can be captured quite promising by using ***MAT_215**. Current investigations focus on failure modelling, especially how to improve the post failure under biaxial loading for shell elements.

Finally, two case studies are shown, both models with over 400.000 elements run as intended and showed good correlation to test results. Further developments focus on the improvement on time step calculation for anisotropic cases, green columns in fig. 22 show first improvements in a current development version.

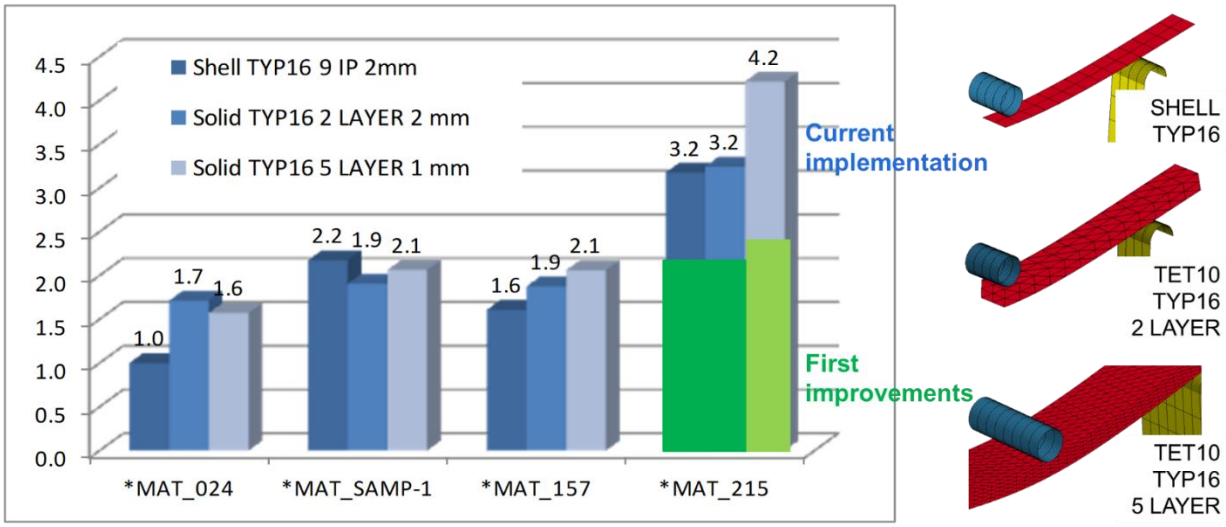

Fig.22: Comparison of CPU-time for different material models and idealizations.

References

[1] Reithofer P., Fertschej, A. Jilka, B.: 4a micromec für die integrative Simulation faserverstärkter Kunststoffe; 11. LS-DYNA Anwenderforum, Ulm 2012

[2] Reithofer P., Fertschej A.: Dynamic Material Characterization Using 4a impetus; Polymer Processing Society Conference 2015 in Graz, AIP Publishing LLC

[3] Reithofer P., Jilka B.: Short and long fiber reinforced thermoplastics material models in LS-DYNA; 13. LS-DYNA Anwenderforum, Bamberg 2014

[4] Haufe A.: Zum aktuellen Stand der Simulation von Kunststoffen mit LS-DYNA, 4a Technologietag - 2014

[5] Erhart A.: Materialmodelle zur integrativen Simulation in LS-Dyna, 4a Technologietag - 2016

[6] Kolling St. et. al.: Current problems in material modeling of polymers: glass-fiber reinforced plastics; LS-DYNA Forum, Filderstadt 2013

[7] Mori T., Tanaka K., Average Stress in Matrix and Average elastic Energy of Materials with misfitting Inclusions, Acta Metallurgica, Vol.21, pp.571-574, (1973).

[8] Tucker Ch. L. III, Liang Erwin: Stiffness Predictions for Unidirectional Short-Fibre Composites: Review and Evaluation, Composites Science and Technology, 59, (1999)

[9] Maewal A., Dandekar D.P.: Effective Thermoelastic Properties of Short-Fibre Composites, Acta Mechanica, 66, (1987)

[10] Eshelby J. D., The determination of the elastic field of an ellipsoidal inclusion, and related problems, Proceedings of the Royal Society, London, Vol.A, No241, pp.376-396, (1957)

[11] http:// micromec.4a.co.at

[12] Bodor Ch. J.: Kopplung µCT und FEM Berechnung, 4a Technologietag - 2014

[13] Mlekusch B.A., Spiegl B., Ableidinger A., A Physically Based Failure Hypothesis for Short-Fibre Reinforced Thermoplastics for Finite-Element-Analysis, 18th World Conf Polymer Processing Society - PPS 18, Guimaraes, Portugal (2002)

[14] Reithofer P. et. al.: Material characterization of composites using micro mechanic models as key enabler; CAE Grand Challenge, Hanau 2016

[15] Mlekusch, B. A.: Kurzfaserverstärkte Thermoplaste, Ph.D. Thesis, Montanuniversität Leoben (1997)

[16] Reithofer P., Fertschej A., Rollant M., Kolling St., Schneider J.: „failure criteria SFRT and LFRT“, crashMAT 2018, Freiburg

[17] Reithofer P., Fertschej A.: Material Models For Thermoplastics In LS-DYNA® From Deformation To Failure, 15th international LS-DYNA Conference, Detroit 2018

[18] Tian. Zao, et.al. – High-dynamic Drop Test for Fiber Reinforced Plastics in Automotive Control Unit, European Dynaforum, Salzburg 2017

[19] R. Steinberger, et.al. Hirtenberger Automotive Group – Considering the Local Anisotropy of Short Fiber Reinforced Plastics, European Dynaforum, Salzburg 2017

[20] Reithofer P., et. al.: „Workshop - Integrative Simulation von kurz- und langglasfaserverstärkten Kunststoffen“, 4a Technologietag 2016

[21] Fertschej A., Reithofer P.: Glasfaserverstärkte Kunststoffe – 4a Software-Tools im Einsatz, 4a Technologietag 2018, Schladming

[22] Reithofer, P., Fertschej, A.: Failure models for thermoplastics in LSDYNA; Polymer Processing Society Conference 2015 in Graz, AIP Publishing LLC

[23] Steinberger R. et al: Lokale Anisotropie in glasfaserverstärkten Kunststoffteilen: Versuch und Simulation an Probekörpern und Bauteilen, 4a Technologietag 2018, Schladming

Appendix – Material Card Input

CARD 1: General Options / Parameter

Card 1	1	2	3	4	5	6	7	8
Variable	MID	MMOPT	BUPD			FAILM	FAILF	NUMINT
Type	A8	F	F			F	F	F
Default	**none**	**0.0**	**0.01**			**0.0**	**0.0**	**1.0**

CARD 2-3: Element Orientation

analogue to LS-DYNA standard anisotropic material cards
may be overwritten by *INITIAL_STRESS_SHELL/SOLID

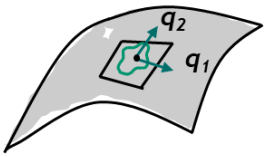

CARD 4: Composite Buildup

exemplary values without any warranty
may be overwritten by *INITIAL_STRESS_SHELL/SOLID

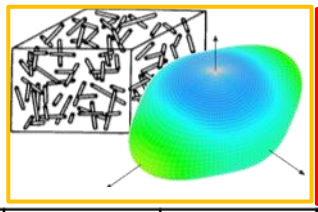

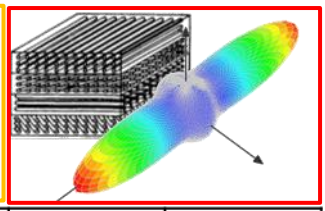

Card 4	1	2	3	4	5	6	7	8
	FVF		FL	FD		A11	A22	
PP GF30	**-0.3**		**200.0**	**10.0**		**0.7**	**0.25**	
PP LGF50	**-0.5**		**1000.0**	**20.0**		**0.65**	**0.30**	
PA6 GF45	**-0.45**		**250.0**	**10.0**		**0.8**	**0.15**	
Carbon UD	**0.6**		**10000.0**	**10.0**		**1.0**	**0.0**	

CARD 5: Fiber Material

Standard values from literature without any warranty

Card 5	1	2	3	4	5	6	7	8
FIBER	ROF	EL	ET	GLT	PRTL	PRTT		
UNITS	kg/mm³	GPa	GPa	GPa	-	-		
glass	**2.59E-6**	**70.0**	**70.0**	**28.8**	**0.217**	**0.217**		
T400	**1.76E-6**	**218.8**	**28.0**	**50.0**	**0.02943**	**0.390**		

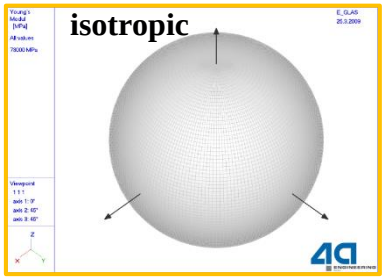

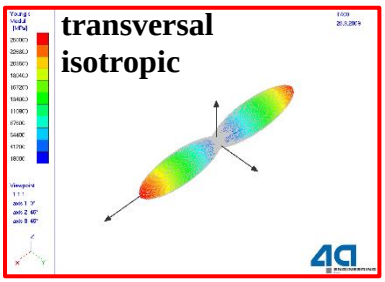

CARD 7: Matrix Material Elasticity

exemplary values without any warranty

Card 7	1	2	3	4	5	6	7	8
Matrix	ROM	E	PR					
Units	kg/mm³	GPa	-					
PP	**0.9E-6**	**1.5**	**0.4**					
PA6 dry	**1.2E-6**	**3.2**	**0.35**					
PA6 cond.	**1.2E-6**	**2.0**	**0.35**					

CARD 8: Matrix Material Visco-plasticity (parameter form)

exemplary values without any warranty

Card 8	1	2	3	4	5	6	7	8
Matrix	SIGYT	ETAN			EPS0	C		
Units	GPa	GPa	-		1/ms	-		
PP	**0.015**	**0.5**			**1.E-6**	**0.10**		
PA6 dry	**0.06**	**1.0**			**1.E-6**	**0.07**		
PA6 cond.	**0.04**	**0.8**			**1.E-6**	**0.10**		

$$\boldsymbol{Hardening}: \boldsymbol{\sigma_{(\varepsilon)} = \sigma_{YT} + E_{TAN} \times \varepsilon_p}$$

$$\textit{Johnson Cook: } \boldsymbol{\sigma_{(\varepsilon,\dot{\varepsilon})} = \sigma_{(\varepsilon)} \times \left[1 + C \times log \frac{max(\dot{\varepsilon},\dot{\varepsilon}_0)}{\dot{\varepsilon}_0}\right]}$$

CARD 9: Matrix Material Tables (table form)

Card 9	1	2	3	4	5	6	7	8
Variable	LCIDT				LCDI	UPF		
Type	F				F	F		
Default	**0.0**				**0.0**	**0.0**		

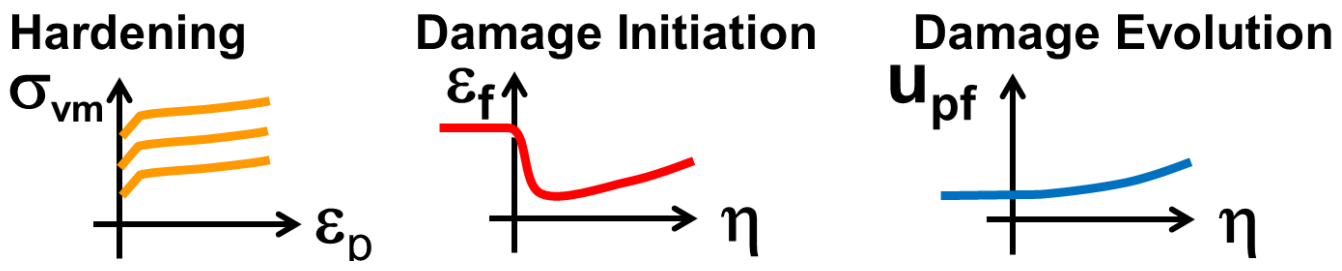

Exemplary Damage Initiation Table3D for SOLID Elements

```
$=========================================================================
$$$ DAMAGE INITATION
*DEFINE_TABLE_3D
$#    tbid
   1000020
$ STRAIN RATE
$#              value      lcid
                0.001   1000121
                  1.    1000122
                1000.   1000123
$=========================================================================
*DEFINE_TABLE_2D
$#    tbid
   1000121
$ LODE ANGLE
$#              value      lcid
                 -1.    1000021
                  1.    1000021
...
$=========================================================================
*DEFINE_CURVE
$ TRIAXIALITY  - EQUIVALENT PLASTIC STRAIN
$     lcid      sidr      scla      sclo      offa      offo    dattyp
   1000021         0       1.0       1.0
$                  x                   y
                -.99                  2.
                -.88                  2.
                -.77                  2.
                -.66                  2.
                -.55                  2.
                -.44                  2.
                -.33                  2.
                -.22                  2.
                -.11                  2.
                   0                  .1
                 .11                  .1
                 .22                  .1
                 .33                  .1
                 .44                 .132
                 .55                 .165
                 .66                 .198
                 .77                  .2
                 .88                  .2
                 .99                  .2
....
```

Exemplary Damage Evolution

```
$=========================================================================
$DAMAGE EVOLUTION
$DAMAGE
*DEFINE_TABLE_2D
$#    tbid
   1000026
$#              value      lcid
                  0.    1000027
                 0.5    1000028
                  1.    1000029
$=========================================================================
$ TRIAXIALIATY - PLASTIC DISPLACMENT
*DEFINE_CURVE
$     lcid      sidr      scla      sclo      offa      offo    dattyp
   1000027         0       1.0       0.0
$                  x                   y
           -1.000000                 .00
...
*DEFINE_CURVE
$     lcid      sidr      scla      sclo      offa      offo    dattyp
   1000028         0       1.0       1.0
$                  x                   y
           -1.000000                 .02
...
*DEFINE_CURVE
$     lcid      sidr      scla      sclo      offa      offo    dattyp
   1000029         0       1.0       1.0
$                  x                   y
           -1.000000                 .05
           -0.660000                 .05
           -0.330000                 .05
           -0.001000                 .05
            0.001000                 .05
            0.330000                 .05
            0.660000                 .05
            1.000000                 .05
$=========================================================================

```

Output: "Plastic Strain" is equivalent plastic strain in matrix.
Extra history variables may be requested for shell elements (NEIPS on DATABASE_EXTENT_ BINARY), which have the following meaning:

Extravar.	DESCRIPTION
1	effs - equivalent plastic strain rate of matrix
2	eta - triaxiality of matrix ... $\eta = -\frac{p}{q}$
3	xi - lode parameter of matrix ... $\xi = -\frac{27 \cdot J_3}{2 \cdot q}$
4	dM - Damage initiation d of matrix (Ductile Criterion)
5	DM - Damage evolution D of matrix
6	RFF - Fiber reserve factor
7	DF- Fiber Damage variable
8	Currently unused
9	A11 - fiber orientation first principal value
10	A22 - fiber orientation second principal value
11	q1/q11
12	q2/q12
13	-/q13
14	-/q31
15	-/q32
16	-/q33
17	FVF- Fiber-Volume-Fraction
18	FL- Fiber length